Suppression of Conducted Emissions in Three-Phase Adjustable Drive Systems

Secil Genc[1], Nur Sarma[2,3], Burcu Gundogdu[4], Okan Ozgonenel[1], Cenk Gezegin[1] and Umit Kemalettin Terzi[5]

[1]Ondokuz Mayis University, Electrical Electronics Engineering Department, Samsun, Türkiye
secil.yilmaz@omu.edu.tr, okanoz@omu.edu.tr, cenk.gezegin@omu.edu.tr
[2]Duzce University, Electrical Electronics Engineering Department, Duzce, Türkiye
[3]Durham University, Department of Engineering, Durham, UK
nursarma@duzce.edu.tr
[4]Hakkari University Colemerik, VHS, Computer Technologies, Hakkari, Türkiye
burcugundogdu@hakkari.edu.tr
[5]Department of Electrical And Electronics Engineering, Faculty of Technology, Marmara University, Istanbul, Türkiye
terzi@marmara.edu.tr

Abstract

The fundamental issue with high switching power converters is electromagnetic interference. The converter design must be electromagnetically compliant for an operation to be secure. Filters play a crucial role in mitigating electromagnetic interference (EMI) within three-phase systems. This paper presents examining the electromagnetic interference associated with a three-phase inverter interconnected to the grid. The reported measurements were taken after the filter and applied with three-phase adjustable drive system for 9-150kHz frequency ranges. Therefore, experimental evidence supports the EMI filter's noise attenuation. In conclusion, the presented study fills in the gaps measuring uncertainties for three-phase emissions, assisting engineers in the design of three-phase converters.

1. Introduction

An inverter is a type of power electronics device that is crucial to the integration of renewable energy plants into grids. Due to its increased power density, great efficiency, and lower cost, grid-connected solar inverters have attracted interest. Modern semiconductor technology allows for the switching of inverter circuit elements at higher frequencies, resulting in high power density and small circuit sizes. High switching rates result in high levels of conducted emissions, which in turn results in EMI as substantial contributors to electromagnetic pollution [1]. This type of pollution possesses the potential to interfere with the functioning of other equipment [2-6]. Industrial product designers are required to provide industrial components are comply with the electromagnetic compatibility (EMC) standards outlined in relevant laws and regulations. Electromagnetic interference (EMI) between 9 kHz and 150 kHz has become a major concern in many industries, especially when it comes to high-power inverters. Switching frequencies of these inverters are normally restricted to a few kHz, leading to EMI emissions to be between 9kHz and 150kHz. It is critical to note that current EMC and power quality standards do not particularly cover this frequency range because there are no standards. EMC standards primarily address lower frequency ranges, whereas power quality standards often concentrate on higher frequency ranges [7-9].

This frequency range gap is closely related to the advancement of technology. The European Committee for Electrotechnical Standardization has released two reports in reaction to this challenge. They have focused on adhering to the requirements given in IEC 61000-2-2 and IEC 61000-2-12, ensuring compatibility between 9 and 150 kHz. It has become a major problem in many areas that there are no defined standards for electromagnetic interference between 9 and 150 kHz in frequency ranges [12]. Power electronics circuits must solve the challenging EMI filter design challenge specifically for their circuit.

It is essential to identify the interference channels in the power electronics application to design a suitable filter. The adjustable speed drive (ASD) used in this study is one of the most widely used applications in contemporary power systems with relatively high electromagnetic emission levels. The analysis of electromagnetic interference (EMI) emissions from a grid-connected adjustable drive system spans the frequency range of 9 to 150 kHz. The design of EMI filters optimized for maximum efficiency in demanding laboratory conditions is also presented in the paper. The analysis of the most effective EMI filter designs for variable speed drive systems operating in the 9–150 kHz frequency range is lacking, despite the lack of research on the subject. The study covers the following topics. In Section II, the suggested system architecture is reviewed and provided. The outcomes of the laboratory study are discussed in Section III. The EMI filter's design is explained in Section IV. In conclusion, this paper is simply summarized.

2. Measurement of Conducted Emissions

The experimental setup aimed to explore the effects of conducted emissions originating from three-phase adjustable drive system connected the main. The set up configuration included a personal computer (PC), an induction motor, a three-phase AC/AC converter, a data collection card (DAQ, NI USB 6210), a three-phase filter, and a line impedance stabilization network (LISN) covering the 9kHz-30MHz frequencies. This test arrangement is illustrated in Figure 1.

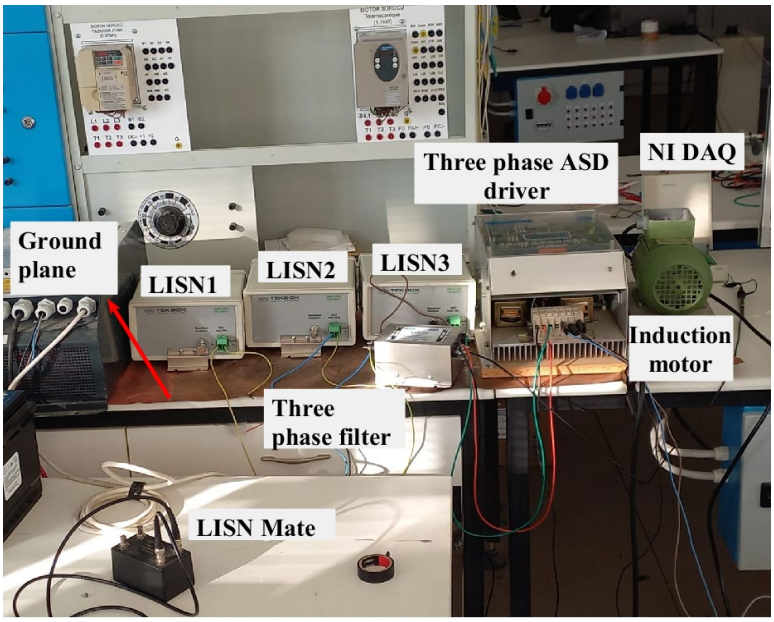

Fig. 1. Test setup of the experimental system

FFT-based MATLAB approach has been used as a substitute for physical receiver in the context of EMI. The suggested emissions measurements from a three-phase converter and filter design are shown in Fig. 2.

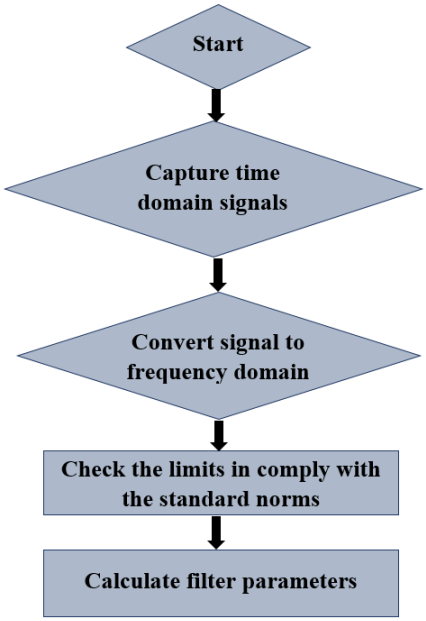

Fig. 2. Flowchart of the system

2.1. Analysis of Conducted Emissions with STFT

Both differential mode (DM) and common mode (CM) signals are captured as time-varying signals. Schematic of CM and DM current separator with LISN is given in Fig. 3.

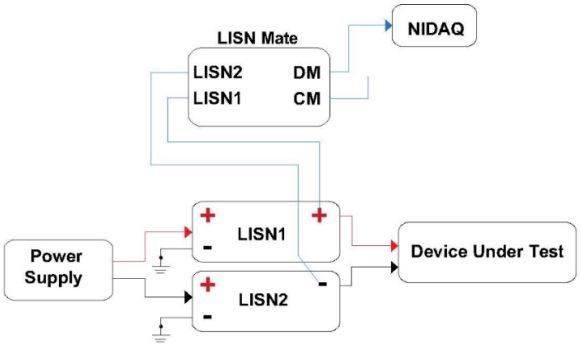

Fig. 3. Schematic of CM and DM current separator with LISN

The harmonic and amplitude characteristics of these EMI disturbances change in time. For the approved EN 50065 standard, which spans 9 to 150 kHz frequency ranges, a 200Hz band has been chosen as the frequency resolution. Then, using FFT, this signal was translated into the frequency domain and contrasted with predetermined bounds [13].

The STFT implementation detail is given in Equation 1.

$$x(t_c, t) = x(t)\omega(t - t_c) \quad (1)$$

The conversion signal is x(t). The center value of the symmetric window function is denoted by t_c. ω is the center frequency of the window. Converted signal is x(t_c, t) The Fourier transform was applied to the divided signal. T The conversion of the STFT values to dBμV, as found in Equation 2, is necessary to compare the measurement outcomes with the recommended standard limits [14].

$$\text{db}\mu\text{V} = 20\log(\text{V} \times 10^6) \quad (2)$$

3. EMI Filter Design and Element Choice

A CM choke, a Y capacitor, and a DM inductor are the components used in the design of an EMI filter for common mode and differential mode, respectively. Each component in an

EMI filter may potentially filter 20dB of noise each decade [15]. Steps of EMI filter design and element choice are as follows.

Step 1: Using Equations (3) and (4), the specifications for CM and DM attenuation are established under the worst possible laboratory circumstances. The standard limit for the necessary maximum attenuation is chosen to be the lowest standard, EN-50065. The noise suppression must be 6dB greater than the surpassing noise due to higher measurements of DM/CM with the disturbance separation compared to the actual values. The cut-off frequency is the highest frequency at which noise starts to be suppressed. Figure 4 displays the filter corner frequency as well as the necessary CM and DM attenuations.

$$Vreq_{CM}(dB\mu V) = V_{CM} - Vlim_{EN50065} + 6 \quad (3)$$

$$Vreq_{DM}(dB\mu V) = V_{DM} - Vlim_{EN50065} + 6 \quad (4)$$

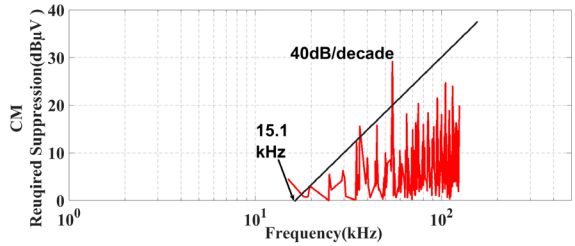

(a)

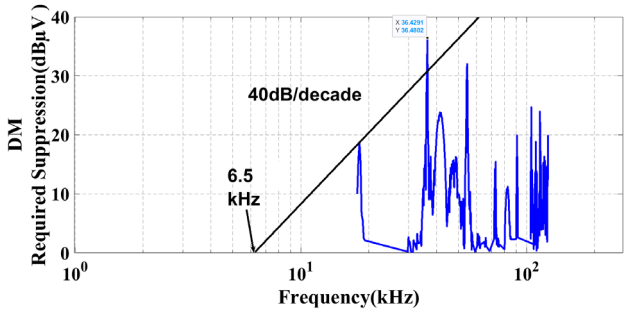

(b)

Fig. 4. Necessary suppression CM and DM

Step 2: The attenuation criteria for Common Mode (CM) and Differential Mode (DM) are ascertained through two specific benchmarks. The reference for the maximum permissible attenuation is defined by the EN-50065 standard. To accommodate potential measurement variations when employing noise separators, a safety margin is incorporated, setting the noise attenuation to be 6dB higher than the exceeded noise level. The target CM and DM attenuations, along with the filter's corner frequency, are visually presented in Fig. 4. The identification of the corner frequency entails graphing a line with a slope of -40dB/decade, drawned the designated noise attenuation curve tangentially. In accordance with the standard graphical technique, the intersection of this line with the horizontal axis establishes the corner frequency. Utilizing this visual approach, the resulting cutoff frequencies are computed as follows: f_{CM} = 15.1kHz for CM noise and f_{DM} = 6.5kHz for DM noise.

Step 3: The corner frequencies of the filter are calculated as follows: L_{CM} component is calculated with Equation (5). Given the safety constraints related to leakage current, the capacitance value Cy is typically restricted to 3.3 nF when considering operations at 50Hz frequency. Therefore, L_{CM} component is calculated as 16.8mH. Lcm is selected as a practical value 7.448mH choke.

$$L_{CM} = \left(\frac{1}{2\pi f_{CM}}\right)^2 \frac{1}{2C_y} \quad (5)$$

Step 4: DM component Cx is calculated with Equation (6).

The stray inductance of a CM coil can operate as a DM coil, potentially negating the requirement for separate DM coils in specific situations. In practice, the value of leakage inductance typically falls within the range of 0.5% to 2% of the combined L_{CM} (inductance-capacitance) value. Consequently, L_{DM} is determined as 1.7% of L_{CM} which is 4.7µF.

$$C_X = \left(\frac{1}{2\pi f_{DM}}\right)^2 \frac{1}{L_{DM}} \quad (6)$$

Briefly, circuit diagram of the EMI filter is given in Fig. 5.

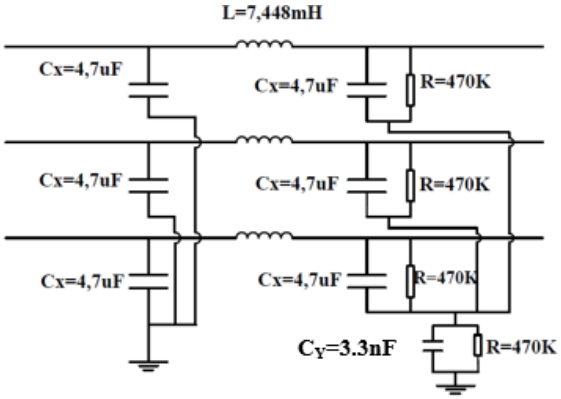

Fig. 5. EMI filter circuit diagram

C_x and L in the circuit diagram attenuate the common mode noise whereas Cy attenuates the differential mode noise. R resistors are used as discharge resistors. Attenuating DM noise can benefit from DM inductance, which is regarded as leakage inductance in CM.

Thus, in this design, the stray inductance of the CM suppresses the DM noise without requiring the use of a separate DM coil.

4. Experimental Results

The three-phase filter was created for 380V/20A in line with the advised standards, as shown in Fig. 6, to meet the frequency range of 9kHz-150kHz, in which the design procedures are explained in Section 2.

Fig. 6. EMI three phase filter application

To assess the noise attenuation capabilities of the filter, we conducted an AC analysis of the equivalent circuit within the PSIM environment, depicted in Figure 7.

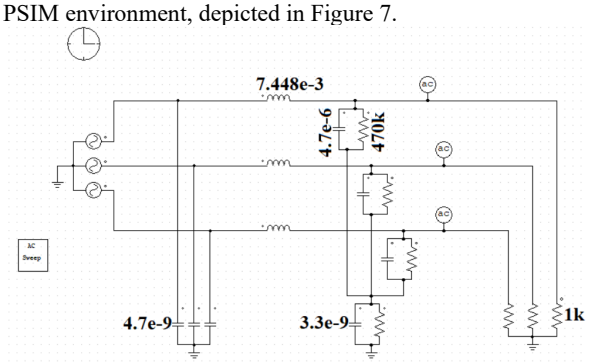

Fig. 7. AC analysis of EMI filter

Figure 8 illustrates the AC analysis of the filter. This circuit permits the transmission of lower frequency power signals while effectively suppressing unwanted higher frequency noise. It attenuates and removes above 10kHz frequencies, and it allows to pass low frequency to provide system operation with 50 Hz. So, this filter has a low pass filter characteristic. The noise suppression of the filter is 30dB below the frequency range of 150kHz. This means that, it provides the required attenuation according to Fig. 4 results. Therefore, based on AC analysis, the filter performs effectively for frequency ranges between 9kHz and 150 kHz.

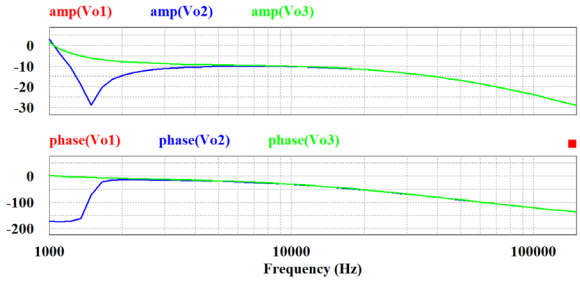

Fig. 8. Result of AC analysis for EMI filter

When a three-phase filter is connected to the system, the CE result is given in Fig. 9. Some standards are suggested to use as a limit for 9kHz-150kHz frequency band ranges. Emission limits for industrial, medical, and scientific equipment are established in accordance with the CISPR 11 standard. In contrast, electrical lighting systems are regulated by the CISPR 15 standard, similar with CISPR 11, often extends its reach to higher frequency ranges.

Active supply transducers find their criteria and operational conditions detailed in IEC TS 62578. Power line communication, whether in general or industrial contexts, is addressed by EN50065, with variations manifesting beyond 100 kHz. EN50160 takes a comprehensive approach, covering characteristics and events related to low, medium, and high voltage power supplies.

Military testing standards, as defined by Mil-Std 461, provide a rigorous framework for evaluating equipment performance for different scenarios. It is important to note that the filter design, as mentioned earlier, places a strong emphasis on strict adherence to the highest standards, particularly focusing on meeting the requirements outlined by EN 500065—the minimum recommended standard. This methodical approach minimizes electromagnetic interference in a variety of applications while also ensuring optimal performance. Based on the experimental findings, the filter complies with the specified suppression levels and does not exceed any standards.

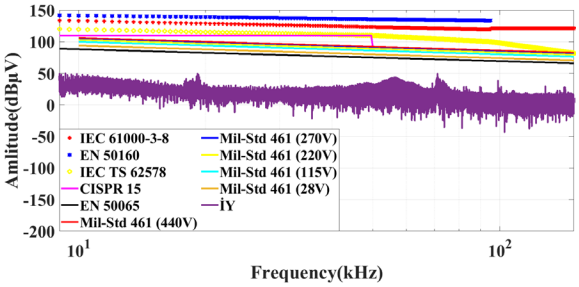

Fig. 9. Suppression of CE

5. Conclusions

Power electronics applications, particularly inverters, present a design challenge for EMI filters. Given the unique nature of each filter design tailored to a specific circuit, it is imperative to perform noise modeling for the associated circuit. This research focuses on delineating the impact of standard three-phase AC/AC converters employed in AC grids for drivers. Installation of the measuring design complies with CISPR 16-1-2 and MIL-STD-461F criteria. A solution strategy to boost power quality is provided based on this converter. This research has concentrated on conducted emissions at frequencies lower than 150kHz because of no standard norms. To ensure the verification design of the EMI filter the experimental study has been carried out. All results undergo systematic experimental testing to demonstrate compliance with the specified limits. The experimental results serve as confirmation of the filter's efficacy. The findings of this study may serve as a guide for the designers.

6. Acknowledgment

This research received backing from Ondokuz Mayis University through Projects PYO.MUH.1904.21.011 and PYO.MUH.1906.21.002. Additionally, the authors express gratitude to Meram Electricity Distribution Company, Grid Innovation Software Technologies, and the Energy Market Regulatory Authority (EMRA) for their valuable contributions and support towards the successful execution of this project.

7. References

[1] H. Hizarci, U. Pekperlak and U. Arifoglu, "Conducted emission suppression using an EMI filter for grid-tied three-phase/level T-type solar inverter", *IEEE Access*, vol. 9, pp. 67417-67431, May 2021.

[2] A. Zeghoudi, A. Bendaoud, H. Slimani, M. Miloudi, H. Miloudi and L. Canale, "Experimental measurements of near magnetic field by different probe for AC/DC LED driver", in *2022 IEEE International Conference on Environment and Electrical Engineering and 2022 IEEE Industrial and Commercial Power Systems Europe (EEEIC/I&CPS Europe)*, Prague, Czech Republic, 2022, pp. 1-6,

[3] R. Smolenski, J. Bojarski, A. Kempski and P. Lezynski, "Time-domain-based assessment of data transmission error probability in smart grids with electromagnetic interference", *IEEE Trans. Ind. Electron*., vol. 61, no. 4, pp. 1882-1890, Apr. 2014.

[4] T. W. Dawson, K. Caputa, M. A. Stuchly, R. B. Shepard, R. Kavet and A. Sastre, "Pacemaker interference by magnetic fields at power line frequencies", *IEEE Trans. Biomed. Eng*., vol. 49, no. 3, pp. 254-262, Mar. 2002.

[5] A. Anderson, D. Marciano, J. Huber, G. Deboy, G. Busatto, and J. W. Kolar, "All- SiC 99.4%- efficient three- phase T- type inverter with DC- side common- mode filter", *Electronics Letters,* vol.59, no. 12, pp. 12821, 2023.

[6] Zeghoudi, L. Canale, A. Bendaoud, A. Tilmatine and G. Zissis,"Experimental measurements of shielding ınfluences on near magnetic field for led lighting sources", in *2023 IEEE International Conference on Environment and Electrical Engineering and 2023 IEEE Industrial and Commercial Power Systems Europe (EEEIC/I&CPS Europe)*, Madrid, Spain, June 2023, pp. 1-6.

[7] P. S. Tomar, M. Srivastava and A. K. Verma, "An improved current-fed bidirectional DC–DC converter for reconfigurable split battery in EVs", *IEEE Trans. Ind. Appl.,* vol. 56, no. 6, pp. 6957-6967, Nov. 2020.

[8] T. Karaca, B. Deutschmann and G. Winkler, "EMI-receiver simulation model with quasi-peak detector", *IEEE Int. Symp. Electromagn. Compat.*, pp. 891-896, 2015.

[9] L. Wan et al., "Limitations in applying the existing LISN topologies for low frequency conducted emission measurements and possible solution", in *Proc. Asia–Pacific Int. Symp. Electromagn. Compat. (APEMC),* pp. 1-4, Sep. 2021.

[10] S. Lodetti et al., "On the suitability of the CISPR 16 method for measuring conducted emissions in the 2–150kHz range in low voltage grids*", Electric Power Systems Research*, vol. 216, pp. 109011, 2023.

[11] A. Mariscotti, "Harmonic and supraharmonic emissions of plug-in electric vehicle chargers", *Smart Cities*, vol. 5, no. 2, pp. 496-521, 2022.

[12] E. Larsson, M. Bollen, M. Wahlberg, C. Lundmark and S. Ronnberg, "Measurements of high-frequency (2–150 kHz) distortion in low-voltage networks*", IEEE Trans. Power Del*., vol. 25, no. 3, pp. 1749-1757, Jul. 2010.

[13] L. Sandrolini and A. Mariscotti, "Signal transformations for analysis of supraharmonic emi caused by switched-mode power supplies", *Electronics*, vol. 9, no. 12, 2020.

[14] L. Ensini, L. Sandrolini, D. W. P. Thomas, M. Sumner and C. Rose, "Conducted emissions on dc power grids", in *2018 International Symposium on Electromagnetic Compatibility (EMC EUROPE),* Amsterdam, Netherlands, Aug. 2018, pp. 214-219.

[15] F. Y. Shih, D. Y. Chen, Y. P. Wu and Y. T. Chen, "A procedure for designing EMI filters for AC line applications", *IEEE Trans. Power Electron*., vol. 11, no. 1, pp. 170-181, Jan. 1996.